New parameters for the characterization of diagenetic alterations and heat-induced changes of fossil bone mineral using Fourier transform infrared spectrometry

M. Lebon [a,b,*], I. Reiche [b], J.-J. Bahain [a], C. Chadefaux [b], A.-M. Moigne [a], F. Fröhlich [a], F. Sémah [a], H.P. Schwarcz [c], C. Falguères [a]

[a] UMR 7194 CNRS – Département de Préhistoire du Muséum national d'Histoire naturelle (MNHN), 1 rue René Panhard, 75013 Paris, France
[b] UMR 171 CNRS – Centre de Recherche et de Restauration des Musées de France (C2RMF), Palais du Louvre, 14 quai François Mitterrand, 75001 Paris, France
[c] School of Geography and Earth Sciences, McMaster University, Hamilton, ON, Canada L8S 4K1

ARTICLE INFO

ABSTRACT

Diagenetic alteration may limit the potential use of the biogenic composition of fossil bone as a reliable source of information for dietary, environmental and climatic reconstructions. One of the key parameters used to determine the state of preservation of fossil remains is their crystallinity. This can be evaluated by means of infrared spectroscopy, measuring the "splitting factor" (IRSF). However, the crystallinity may fail to describe the extent of chemical and mineralogical changes occurring during fossilization, and cannot be used alone as a reliable indicator of biogenic signal preservation.

In this study, modern bones were experimentally heated in order to monitor the changes of FTIR spectral features related to an evolution of mineral properties. Further spectroscopic proxies of the mineral composition and structure were defined and calibrated. This method was then applied on unburnt, charred and calcined bones coming from three archaeological sites (Bize-Tournal, Organc 3 and Song Terus).

The results obtained on modern and fossil bones demonstrate that low temperature heating and diagenetic processes may induce similar effects on bone mineral, while these processes are clearly distinct from those occurring during high temperature heating (>550 °C). The comparison between charred and calcined fossil bones shows that heating over 550 °C reduces the reactivity of the mineral phase and prevents compositional and structural characteristics from experiencing diagenetic modification.

Applied to unburnt fossil bones, the proxies developed in this study, easily obtained from FTIR spectra, provide a more reliable evaluation of the degree of preservation than IRSF alone and contribute to a better understanding of the diagenetic processes.

© 2010 Elsevier Ltd. All rights reserved.

1. Introduction

The elemental and isotopic mineral compositions of paleontological remains like bones and teeth represent an important source of information for reconstructing ancient climates, past environments, and species diet or migration (Lee-Thorp, 2002). Indeed, bone is a complex tissue mainly composed of a mineral phase intimately associated with a collagen matrix. The chemical composition and the structure of the mineral phase are close to hydroxyapatite ($Ca_{10}(PO_4)_6(OH)_2$; HA) but differ from it in their non-stoichiometric composition and the presence of ionic substitutions in different crystallographic sites (LeGeros, 1981). Hence, phosphate ions are largely substituted by carbonate (CO_3^{2-}) and/or acid phosphate (HPO_4^{2-}) (LeGeros, 1981; Legros et al., 1987). These substitutions create large distortions and strains in the mineral lattice leading to an enhancement of the dissolution rate and a limitation of the crystallite size (LeGeros, 1981; Wopenka and Pasteris, 2005).

In bones, apatite crystals generally have a maximum length ranging from 15 to 200 nm and a thickness between 2 and 6 nm (Chadefaux and Reiche, 2009; Currey, 2006; Elliott, 2002; Eppell et al., 2001). One of the most important properties of these nanocrystallites is their high specific surface area. The existence of a hydrated layer on the nanocrystallite surface may also contribute to their reactivity (Rey et al., 1990, 1991). This hydrated layer is characterized by bivalent ions as Ca^{2+}, HPO_4^{2-} and CO_3^{2-} residing in

so-called "non-apatitic environments", corresponding to less stable locations than in the apatitic lattice (Eichert et al., 2005; Rey et al., 2007, 1990, 1991).

Different post-mortem processes may strongly affect the structure and chemical composition of bones after their exposure to soil environments during burial. Such processes, caused by microbial activity or environmental physico-chemical conditions such as groundwater pH or sediment composition, may rapidly lead to the partial or complete degradation of organic matter (mainly collagen) and to its leaching by groundwater (Collins et al., 2002). Increase of the bone porosity due to loss of organic matter allows interactions of bone components with groundwater and promotes the uptake of exogenous chemical elements (fluoride [F$^-$], uranyl [UO$_2^{2+}$], rare earth elements [REE], etc.), and precipitation of secondary minerals (calcite, pyrite, barite, etc.). This process of transformation of bone mineral can to some extent be monitored by measurement of the so-called crystallinity, to be discussed below, a parameter reflecting the degree of perfection of the lattice, and the crystal size, as a result of dissolution/recrystallization processes (Collins et al., 2002; Hedges, 2002; Hedges and Millard, 1995; Reiche et al., 1999, 2003; Trueman et al., 2008). Some of these diagenetic processes are critical to geochronological methods such as U-series and ESR dating (Grün, 1989; Schwarcz, 1997), but most of them may modify the original elemental or isotopic signals recorded *in vivo*. The ionic exchanges between bone mineral and groundwater could affect more particularly the original isotopic composition of structural carbonate (δ^{13}C, δ^{18}O) and phosphate (δ^{18}O) in bioapatite, limiting the usefulness of fossil bones as a source of information to reconstruct climates or diets (Bocherens et al., 2008; Lee-Thorp, 2002).

Due to the importance of the preservation of the original biochemical signal for archaeological and paleontological analytical purposes, different techniques have been applied to investigate fossilization processes and to measure the extent of *post-mortem* changes in bones over geological times. A set of indices has been developed to estimate the alteration degree of bones, using either the degradation and loss of collagen (Chadefaux et al., 2009; Collins et al., 2002; Nielsen-Marsh et al., 2000), the preservation of histological structures, or the increase of porosity (Hedges et al., 1995; Jans et al., 2002; Turner-Walker and Syversen, 2002) and crystallinity (Berna et al., 2004; Person et al., 1995; Weiner and Bar-Yosef, 1990).

2. Mineral crystallinity as measured by infrared spectrometry

Fourier transform infrared spectroscopy (FTIR) constitutes an efficient tool to assess both the composition and the structure of the organic and mineral phases of fossil bones. This technique has thus been widely applied in this way to detect diagenetic changes in collagen and carbonate contents.

Termine and Posner (1966) suggested the use of the degree of splitting of one of the phosphate absorption bands in the HA spectrum (near 590 cm^{-1}) to measure the crystallinity. They developed this method to measure the degree of crystallization in poorly crystalline hydroxyapatite. Weiner and Bar-Yosef (1990) further suggested that this parameter reflected both the perfection of the HA crystal lattice and the crystal size. Many subsequent authors have explored the use of this method including Shemesh (1990), Wright and Schwarcz (1996), Sponheimer and Lee-Thorp (1999), and Surovell and Stiner (2001). This IR crystallinity index (called splitting factor, IRSF) is one of the most widely used parameters to estimate the diagenetic alteration. However, some studies have suggested that crystallinity values are influenced by sample preparation (Nakano et al., 2002; Surovell and Stiner, 2001). Moreover, recent works have shown that the splitting factor used

alone may fail to describe adequately the complexity and heterogeneity of diagenetic processes and cannot be used as an unambiguous indicator of biogenic signal preservation in the mineral matter (Lee-Thorp and Sponheimer, 2003; Pucéat et al., 2004; Reiche et al., 2003; Trueman et al., 2008).

Fourier transform infrared spectroscopy can also be applied to investigate variations in the chemical environments of molecular species in both biological and synthetic apatites using some absorption bands specific to PO$_4^{3-}$ and HPO$_4^{2-}$ groups in apatitic and non-apatitic environments (Cazalbou et al., 2004; Miller et al., 2001; Rey et al., 2007, 1990).

In this paper, such analytical approaches, previously applied on biological apatites, are used to study the mineral phase modifications during diagenesis in order to develop further indices of bone alteration. For this purpose, the $\nu_1\nu_3$PO$_4$ domain extending between 1200 and 900 cm^{-1} was investigated to obtain information on phosphate ion environments. These data have been compared to crystallinity measurements (IRSF), carbonate content and collagen loss derived from FTIR spectra, as well as to trace element composition obtained from particle induced X-ray and gamma emission micro-analyses (μPIXE/PIGE).

Both burnt and unburnt, modern and archaeological bones were studied. Comparison between such samples appears to be a helpful way to understand the diagenetic processes. Indeed, even though heating and diagenesis are two different processes, an experimental heating of modern bones reproduces in a short time some effects similar to diagenetic processes that occur over geological time, e.g. crystallinity increase (Munro et al., 2007, 2008; Person et al., 1996). Furthermore, recrystallization that occurs during heating improves the stability of the mineral phase. Thus, calcined bones heated at temperature higher than 700 °C are much less sensitive to diagenetic alterations than unburnt or charred samples (Lanting et al., 2001; Lebon, 2008; Reiche et al., 2002a). Such intensely heated bones can constitute a reference sample representing a diagenetically unaltered state and contribute to the understanding of diagenetic processes, which affect fossil bones in sedimentary, taphonomical or archaeological contexts.

3. Material and methods

3.1. Experimental modern material

The diaphysis of the humerus of a mature ox was defleshed. The cortical part was crushed and sieved to select grains ranging from 1.25 to 2 mm. This sample was then split into 23 aliquots weighing 0.75 g each. These aliquots were heated for 60 min at temperatures ranging from 120 to 900 °C in an oven in air, and then cooled down quickly at room temperature. The oven was heated to the required temperature prior to emplacement of the samples, and the heating temperatures were then monitored and stabilized at ±1 °C. The temperature steps were 20 °C from 120 to 280 °C, and 50 °C between 300 and 900 °C. Additional unheated aliquots were used as comparisons.

3.2. Archaeological material

Bone samples from three archaeological Pleistocene sites were examined: Bize-Tournal Cave (Aude – France), Orgnac 3 (Ardèche – France) and Song Terus Cave (Java – Indonesia). For these archaeological sites, both unheated and burnt bones were analyzed. These samples were classified prior to infrared analysis on the basis of their macroscopic features according to color modifications observed on the modern reference. Thus, the category "UnH" corresponds to samples without clear heating indicators (0–240 °C – unheated). The category "Cha" corresponds to samples showing char stains or

complete charring (260–450 °C – charred). Samples partially or completely calcined (500–900 °C) were grouped in the "Cal" category. All samples selected here present an unambiguous burning state. After surface cleaning, a few milligrams of each fossil bone were sampled for FTIR analysis. Sampling was done locally in very homogeneous areas to avoid any heterogeneity of composition.

The first set of fossil samples was composed of 23 fragments of bones of unidentified mammals (probably reindeer (*Rangifer tarandus*)) recovered from a Magdalenian level of the Bize-Tournal Cave, dated to 14 700 ± 700 years BP (Tavoso, 1987). The surface preservation of these bones appeared excellent (Magniez, 2009) and previous FTIR analyses have shown partial collagen preservation (Lebon, 2008).

The second set of fossil remains was made up of 17 samples from the Orgnac 3 Acheulian site. These samples came from archaeological levels 2 and 6, dated respectively to 330 and 360 ka (Falguères et al., 1988). These samples appeared macroscopically more altered than those from Bize-Tournal.

The last set of samples comprised 26 specimens from the "Tabuhan" layers of the Song Terus Cave, dated between 30 and 80 ka (Hameau et al., 2007; Sémah et al., 2004). The Song Terus Cave is located near the southern coast of East Java, and therefore submitted to a seasonal tropical climate characterized by high moisture and high average annual temperature. These samples clearly differed from those from the two previous sites by significant surface alterations and deposits of manganese oxides.

3.3. Fourier transform infrared spectroscopy (FTIR) analyses

3.3.1. Sample preparation

A few milligrams of each sample were ground in acetone to obtain a grain size smaller than 5 μm. KBr pellets were prepared by mixing 2.5 ± 0.1 mg of bone powder with ca. ~1 g KBr. 300 mg of this mixture was compressed at 11 t/cm^{-1} for 1.5 min following the protocol described by Fröhlich (1989). Infrared spectra were collected using a Bruker Vector 22 FTIR spectrometer by accumulation of 64 scans with a resolution of 2 cm^{-1}.

3.3.2. Composition monitoring

3.3.2.1. Classical indices.
The mineral composition was monitored using carbonate and phosphate vibration bands. Relative carbonate content was estimated from the ratio between the absorbance of the $\nu_3 CO_3$ band at 1415 cm^{-1} and the $\nu_3 PO_4$ band around 1045 cm^{-1} (Fig. 1a) (Wright and Schwarcz, 1996). The splitting factor (IRSF) was measured from the two anti-symmetric bending vibration bands of phosphate ($\nu_4 PO_4$) at 565 and 605 cm^{-1} (Fig. 1b) following the method of Weiner and Bar-Yosef (1990), using a baseline drawn between 495 and 750 cm^{-1}. The peak intensity ratio between the Amide I band at 1660 cm^{-1} band and the $\nu_3 PO_4$ band around 1045 cm^{-1} was also used to evaluate collagen preservation in fossil bones.

3.3.2.2. $\nu_1\nu_3 PO_4$ domain.
The $\nu_1\nu_3 PO_4$ domain consists of an intense and broad band extending between 900 and 1200 cm^{-1} and results from symmetric (ν_1) and anti-symmetric (ν_3) P–O stretching vibrations (Fig. 1c). Other studies that focused on biological or synthetic apatites have revealed that this broad domain is composed of several underlying components indicative of the mineral composition (Gadaleta et al., 1996; Rey et al., 1991). Some sub-bands have thus been assigned to phosphate ions in stoichiometric, non-stoichiometric apatite or to acid phosphate (HPO_4^{2-}) ions (Gadaleta et al., 1996; Paschalis et al., 1996; Rey et al., 1991). Vibration bands associated with phosphate groups located in apatitic environments (stoichiometric or not) are mainly assigned to the 1020–1100 cm^{-1} spectral domain, while non-apatitic environments and HPO_4^{2-} mostly correspond to the 1100–1200 cm^{-1} spectral domain (Fig. 1c). It has also been reported that the 1030 cm^{-1} component is indicative of phosphates in stoichiometric apatites, whereas the 1020 cm^{-1} region is indicative of non-stoichiometric apatites containing CO_3^{2-} and/or HPO_4^{2-} (Gadaleta et al., 1996; Paschalis et al., 1996; Rey et al., 1991). The 1030/1020 cm^{-1} sub-band ratio is thus commonly used to evaluate mineral crystallinity using IR micro-spectrometry (Gadaleta et al., 1996; Paschalis et al., 1996). Furthermore, several band positions can supply information about the composition and the perfection of the
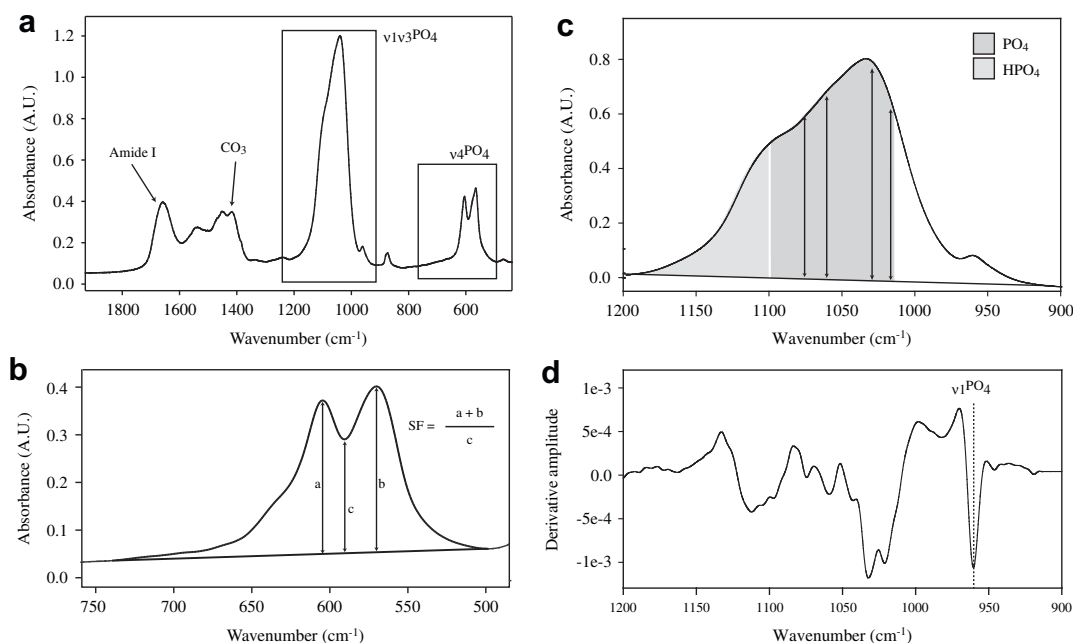

Fig. 1. a) Typical FTIR spectra of fresh bone and localisation of the amide I, carbonate, ν_4 and $\nu_1\nu_3$ phosphate bands. b) IRSF calculation procedure following Weiner and Bar-Yosef (1990). c) Intensity and area used to calculate 1030/1020 and 1060/1075 crystallinity indices and HPO$_4$/PO$_4$ area ratio. d) Second derivative spectra of the $\nu_1\nu_3 PO_4$ domain and localisation of the $\nu_1 PO_4$ component.

mineral phase (Boskey and Pleshko-Camacho, 2007; Gadaleta et al., 1996; Paschalis et al., 1996; Rey et al., 1991). This spectral domain allows us to evaluate the crystallinity, the non-apatitic domain extent and the molecular order within the mineral lattice.

3.3.2.3. Indices obtained from the $\nu 1 \nu_3 PO_4$ domain. In this study, the 1030/1020 ratio was calculated from the ratio of the absorbance intensity at 1030 and 1020 cm^{-1} relative to a baseline between 900 and 1200 cm^{-1} (Boskey and Pleshko-Camacho, 2007; Paschalis et al., 1996). Another crystallinity index, the 1060/1075 cm^{-1} ratio, was also tested and compared to the 1030/1020 ratio and the IRSF value. Acid phosphate content was evaluated from the area ratio of the spectral domain between 1020 and 1100 cm^{-1} (PO$_4^{3-}$ in apatite) and 1100–1150 cm^{-1} (HPO$_4^{2-}$ in non-apatitic environments). The calculation procedure for these different indices is presented in Fig. 1c. The use of the peak intensity ratio to measure the 1030/1020 and the 1060/1075 crystallinity indices was preferred to the deconvolution procedure because peak intensity ratios are linearly correlated to area ratios obtained by curve fitting. Moreover, intensity ratios provide more rapid and more reproducible measures than using deconvolution procedure (Boskey and Pleshko-Camacho, 2007; Lebon, 2008).

The position of the $\nu_1 PO_4$ band centered near 961 cm^{-1} was monitored from second derivative spectra (7-points Savisky–Golay algorithms), to avoid any baseline effects and to measure more accurately the position of this poorly resolved peak (Fig. 1d). Here, the second derivative was preferred to the fourth derivative to avoid the possible presence of artificial bands that have been observed in a previous paper (Lebon et al., 2008).

The reproducibilities of these indices were evaluated from experimentally heated modern samples. For all the temperature steps previously mentioned, three additional aliquots were separately heated and prepared for FTIR measurements as described in a previous study (Lebon, 2008). The mean reproducibilities measured for UnH, Cha and Cal categories are presented in Table 1. These reproducibilities take into account grinding and weighing of pellet preparation as well as infrared spectra acquisition and measurement of indices.

3.4. Micro-PIXE–PIGE analyses

The chemical composition of several representative samples was determined by proton induced X-ray emission (PIXE) and gamma emission (PIGE) spectroscopy. Analyses were performed on bone transversal sections using the external proton microbeam line of the tandem particle accelerator "AGLAE" at C2RMF in the Louvre Museum (Paris – France). Technical details on the accelerator facility are presented in Calligaro et al. (2004). Elemental concentration and statistical errors on the measurements were calculated from PIXE spectra with the GUPIX software described in Maxwell et al. (1988). Fluorine content was quantified by means of micro-PIGE analyses using the net peak areas of the 110 and 197 keV lines

produced by nuclear reactions compared to those determined under the same conditions in fluorapatite (FA) reference samples (Reiche et al., 1999).

4. Results

4.1. Modern samples

4.1.1. Crystallinity

Crystallinity values obtained from IRSF, 1030/1020 and 1060/1075 ratio measurements are listed in Table 2 and plotted on Fig. 2a. Infrared SF and 1030/1020 values for unheated sample were close to those usually noted for mature *in vivo* bone. During heating, these three crystallinity indices show the same trend. The 1030/1020 and 1060/1075 indices were clearly correlated to IRSF ones, respectively with $r^2 = 0.94$ and $r^2 = 0.98$ ($p < 0.001$). A slight increase of crystallinity occurred between 120 and 300 °C, followed by lower values observed from 300 to 400 °C. However, these variations are low considering the standard error measured for the IRSF in this temperature range (± 0.1). Surovell and Stiner (2001) have suggested that such a decrease of IRSF value around 400 °C can be ascribed to the grinding procedure used for FTIR pellet preparation. Above 600 °C, all crystallinity parameters significantly increase as reported by other authors (Munro et al., 2007, 2008; Person et al., 1996; Stiner et al., 1995).

4.1.2. Carbonate and acid phosphate contents

The variation of carbonate and acid phosphate contents into heated samples are listed in Table 2 and illustrated in Fig. 2b. The carbonate/phosphate ratios decrease gradually from 200 to 600 °C, and then drop to minimal values above this temperature. The acid phosphate content slightly decreases between 0 and 300 °C, then remains stable until 600 °C. Above 600 °C, it decreases by a factor of five. Bones heated at temperatures equal to or higher to 650 °C retain only low amounts of carbonate and acid phosphate.

4.1.3. Position of the $\nu_1 PO_4$ vibration band

The sub-band centered around 961 cm^{-1} results from a symmetric P–O stretching vibration (Gadaleta et al., 1996). It presents a positive shift in frequency with temperature increase (Fig. 3a and Table 2). The position of this band gradually increases from 960 $\pm$ 0.2 cm^{-1} for the unheated sample to 963 $\pm$ 0.2^{-1} for samples heated to 650 °C. A strong correlation was found between heating stage and peak position for this temperature range ($r^2 = 0.90$; $p < 0.001$).

4.2. Archaeological material

The FTIR results for archaeological samples are summarized in Table 3. Results for crystallinity (IRSF), $\nu_1 PO_4$ position, carbonate, acid phosphate and collagen contents are plotted in Fig. 4 according to their suspected burning state and in comparison with modern bones for the same stage (i.e. "UnH" unheated or low heating (<260 °C), "Cha" charred (260–450 °C), "Cal" calcined (500–900 °C).

4.2.1. Crystallinity

Archaeological bones from Bize-Tournal and Orgnac 3 sites always reach higher IRSF values than unheated modern bones (Fig. 4a). Crystallinity values for seemingly unheated bones from these two sites are homogeneous and range between 3.5 and 3.8. On the other hand, IRSF values of unheated and charred bones from Song Terus Cave present much more dispersed IRSF values (varying from 3.1 to 4.6). Some of them present crystallinity values equivalent to those of modern bone whereas others show higher

Table 1
Mean values and standard error ($\pm 1\sigma$) of IR indices measured for unheated (UnH), charred (Cha) and calcined (Cal) modern bones.

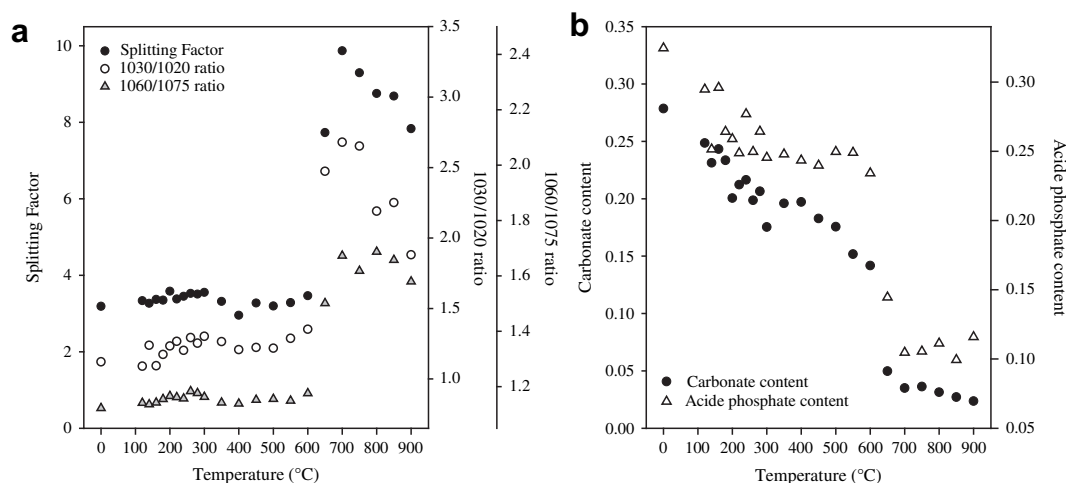|	UnH (120–240 °C)		Cha (260–450 °C)		Cal (500–900 °C)	
IRSF	3.4	±0.1	3.4	±0.1	7.1	±0.3
1060/1075	1.16	±0.01	1.17	±0.01	1.52	±0.05
1030/1020	1.21	±0.04	1.27	±0.02	2.01	±0.08
HPO$_4$ content	0.28	±0.01	0.27	±0.01	0.16	±0.01
$\nu_1 PO_4$ position	960.6	±0.2	961.1	±0.1	962.7	±0.2
CO$_3$ content	0.22	±0.01	0.19	±0.01	0.07	±0.01
Collagen content	0.3	±0.01	–		–	

Fig. 2. a) Crystallinity increase during heating, monitored both by 1030/1020 ratio, 1060/1075 ratio and IRSF. b) Acid phosphate and carbonate contents decrease during experiment.

crystallinity. These bones are clearly poorly preserved, suggesting they underwent more complex diagenetic processes than these of two other studied sites.

Fig. 5 displays the relationship between the splitting factor and the crystallinity indices based on the $\nu_1\nu_3PO_4$ domain. The statistically significant linear relationship between the 1060/1075 ratio and IRSF, which was found for modern samples, is also confirmed for fossil bones ([1060/1075] = 0.086 IRSF + 0.865; Fig. 5b). The relationships between the 1030/1020 ratio and the IRSF for fossil bones slightly differ from those observed for modern samples (Fig. 5a). This is particularly evident for the Song Terus samples for which no correlation is found between IRSF and 1030/1020 ratio. These samples have been excluded from the computation of the IRSF to 1030/1020 regression.

4.2.2. Carbonate and acid phosphate contents

Carbonate content values determined for unheated and charred archaeological bones fluctuate between 0.35 and 0.15 (Fig. 4b).

Table 2
Values of spectroscopic indices measured for modern samples of unheated and heated bones between 120 and 900 °C.

Temperature (°C)	CO_3 content	IRSF	1030/1020	1060/1075	HPO_4 content	ν_1PO_4 (cm^{-1})
0	0.28	3.2	1.12	1.12	0.32	960.0
120	0.25	3.3	1.09	1.14	0.32	960.1
140	0.23	3.3	1.24	1.14	0.27	960.5
160	0.24	3.4	1.09	1.14	0.32	960.1
180	0.23	3.3	1.17	1.16	0.28	960.3
200	0.20	3.6	1.23	1.17	0.28	960.8
220	0.21	3.4	1.27	1.16	0.26	960.7
240	0.22	3.4	1.20	1.16	0.30	960.7
260	0.20	3.5	1.29	1.18	0.27	960.9
280	0.21	3.5	1.25	1.18	0.28	960.8
300	0.18	3.6	1.30	1.16	0.26	961.1
350	0.20	3.3	1.27	1.14	0.26	961.1
400	0.20	3.0	1.21	1.14	0.26	960.9
450	0.18	3.3	1.22	1.15	0.25	961.4
500	0.18	3.2	1.22	1.16	0.27	961.4
550	0.15	3.3	1.29	1.15	0.26	961.8
600	0.14	3.5	1.35	1.18	0.25	962.5
650	0.05	7.7	2.47	1.50	0.15	963.1
700	0.04	9.9	2.68	1.67	0.11	963.1
750	0.04	9.3	2.65	1.62	0.11	963.0
800	0.03	8.8	2.19	1.69	0.11	963.0
850	0.03	8.7	2.25	1.66	0.10	962.7
900	0.02	7.8	1.88	1.58	0.12	962.6

Archaeological samples display more variable amounts of carbonate than modern bones according to their heating categories. For unheated and charred samples from Bize-Tournal, carbonate contents decrease moderately and most samples show values similar to the modern specimens. The Song Terus samples present the largest range of carbonate content particularly for unheated bones.

Calcined samples characterized by high crystallinity (IRSF > 6) are slightly affected by carbonate content modifications.

The acid phosphate content appears to be modified by the geochemical history. All unburnt and charred fossil samples present lower HPO_4^{2-} contents than the modern bones studied here (Fig. 4c), but are similar to HPO_4^{2-} contents of mildly heated modern bones. Acid phosphate contents are more modified for samples from Orgnac 3. Most of the unheated and charred samples from Song Terus present lower HPO_4^{2-} contents than observed in modern samples for these categories. Calcined bones display less modification of their acid phosphate content than for other categories.

4.2.3. Position of the ν_1PO_4 vibration band

Concerning the ν_1PO_4 band frequency, the values of archaeological samples are higher than those for fresh bones (i.e. >960 cm^{-1}), particularly for unheated and charred samples (Fig. 4d). For these two categories, the mean position of this band observed for Bize-Tournal samples is only +0.5 cm^{-1} higher than for modern bones, but a more important shift of +1–1.5 cm^{-1} occurs for the Orgnac bones. These position shifts are significant compared to standard error (±0.2 cm^{-1}). Higher frequencies are observed for unheated and charred bones from Song Terus where the ν_1PO_4 position can exceed that recorded for modern experimentally heated samples.

The frequency of the ν_1PO_4 band is less modified for calcined fossil bones than unheated and charred samples and remains in the range observed for modern bones.

4.2.4. Chemical composition determined by micro-PIXE/PIGE

Elemental concentrations were measured along profiles on bone sections by micro-PIXE/PIGE and the related mean concentrations are summarized in Table 4. Exogenous elements such as Al, Si, Mn, Fe, Cu and Ba are present at relatively high concentrations in archaeological bones. The concentrations of biologically active elements like Na^{2+}, Mg^{2+}, Zn^{2+}, Sr^{2+}, Cl^- and F^-, present in fresh bones, are variable in fossil specimens. The Na^{2+} and Mg^{2+} concentrations are lower in fossil bones than in modern samples.
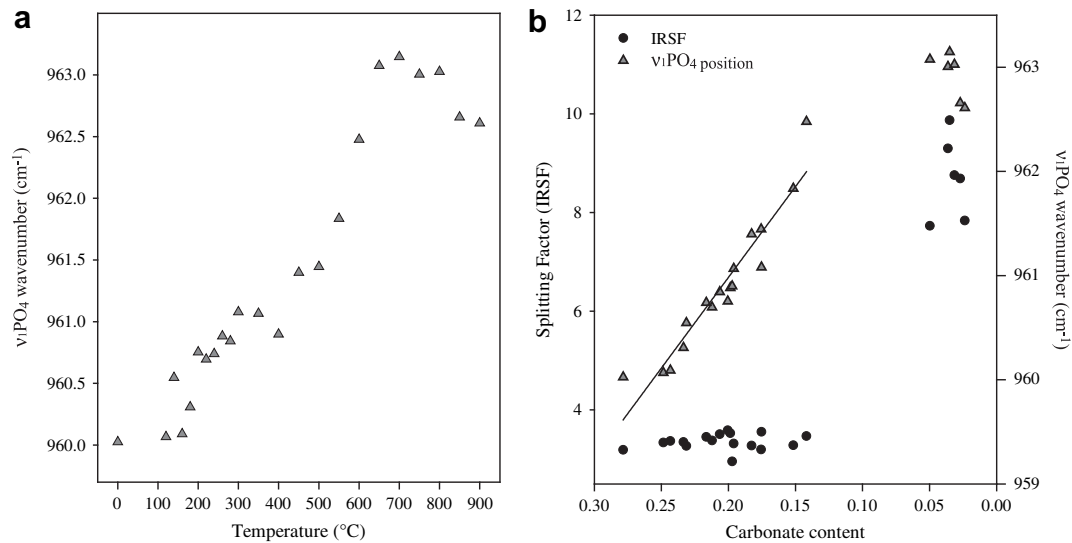
Fig. 3. a) Positive position shift of the v_1PO_4 during heating experiment. b) Positive position shift of the v_1PO_4 and IRSF increase related to carbonate loss during experimental heating. The position shift is linearly correlated to the carbonate loss for samples heated up to 600 °C ($r^2 = 0.90$, $p < 0.001$).

Sr^{2+} and F^- uptakes can be observed in the archaeological samples. At Song Terus, the element composition is strongly affected and the F^- content of some of these samples reaches a mean value around 1.5 %wt. Highly crystallized calcined samples (Org-8 and ST-Ta-3) do not show such extensive alterations of their elemental composition.

5. Discussion

5.1. Modifications of modern bone mineral phase during heating

The FTIR data obtained for experimental samples were used to compare the information on heat-induced modifications provided by different indicators of the composition and the structure of the bone mineral phase.

As previously reported, carbonate ions are an extensive source of strain in the apatite structure and crystallinity increases during heating due to their progressive loss (Biltz and Pellegrino, 1983; Holcomb and Young, 1980). This loss of carbonate leads to an amelioration of the mineral lattice order that becomes negligible beyond 600–650 °C. It therefore allows the growth of crystallites as highlighted by the sharp rise of IRSF values (Pasteris et al., 2004; Rogers and Daniels, 2002). The correlation observed between IRSF, 1030/1020 and 1060/1075 ratios demonstrates that it is possible to measure the crystallinity using either the v_4 or $v_1v_3PO_4$ domains of the FTIR spectra of fossil bones.

The acid phosphate content also decreases during heating but at a lower rate than the carbonate loss, and occurs in two steps. The first step takes place between 120 and 300 °C and might be ascribed to the drying of the mineral phase. The second drop, more significant, occurs simultaneously with increased crystal growth, starting at 550 °C. This major loss of acid phosphate could correspond to the decrease of the specific surface (surface/volume ratio) owing to the crystal growth and the internal re-arrangement of the mineral phase observed over this temperature range.

The shift in position of the v_1PO_4 band provides accurate information about the mineralogical modifications induced by heating. In FTIR spectroscopy, vibrational frequencies are related to the molecular organization within the mineral lattice, hence suggesting that the observed frequency shifts reflect modifications in the phosphate ion environment during heating. Such modifications

have been reported elsewhere by XRD Rietveld analyses, revealing changes of "a" and "c" crystalline parameters at temperatures lower than 600 °C (Etok et al., 2007; Rogers and Daniels, 2002). These changes have been attributed to the exclusion of substituted foreign ions from the mineral lattice. The shift of this v_1PO_4 band seems linearly correlated with the carbonate loss for samples heated up to 600 °C ($r^2 = 0.90$, $p < 0.001$; Fig. 3b). Previous papers have reported such differences in the band position for carbonate hydroxyapatite compared with pure hydroxyapatite (Rey et al., 1991).

In this study, the position of the v_1PO_4 band observed for fresh and low-temperature heated bones were close to those recorded for carbonate hydroxyapatite. On the contrary, the higher position of this band for the samples heated beyond 600 °C corresponded to that observed in carbonate-free HA (Pasteris et al., 2004; Rey et al., 1991). As the carbonates cause a large structural disorder in the mineral lattice of apatite, our results suggest that the position of this band reflects the improvement of lattice order in the bone mineral phase due to heating.

One of the most interesting aspects of these results is that the position shift of the v_1PO_4 band during heating was more sensitive than IRSF to carbonate loss, and induced modifications of phosphate ion environments within the apatite lattice (Fig. 5). According to these results, it seems that the IRSF refers more to crystal size, while the position of the v_1PO_4 bands seems to be more appropriate to describe the lattice strain changes resulting from modifications of the mineral composition.

5.2. Modifications of bone mineral during diagenesis

The results obtained on fossil bones including the crystallinity, the acid phosphate and carbonate contents, and the position of the v_1PO_4 band, provide new insights into diagenetic processes and into the ability of these parameters to evaluate the preservation state of fossil bone mineral.

5.2.1. Crystallinity modifications during diagenesis and limits of IRSF to provide a reliable proxy of alteration state

The crystallinity of the unheated samples from Bize-Tournal and Orgnac 3 sites was higher than for modern bones. However, despite their age differences, these archaeological samples presented very

Table 3

List of archaeological samples analyzed in this study. Heating stages have been established from their macroscopic characteristics (unheated or exposed to low temperatures (category "UnH"); partially or completely charred (category "Cha"); partially or completely calcined (category "Cal")). Collagen and carbonate content correspond respectively to the intensity ratio of the Amide I- and CO_3/PO_4 bands. "−" refers to the absence of detectable Amide I band. Acid phosphate content in the sample was estimated from the ratio of the integrated area of HPO_4 and PO_4 domains.

| Sample	Site	Layer	Age	Heating stade	Collagen content	CO_3 content	IRSF	1030/1020	1060/1075	HPO_4 content	$\nu 1PO_4$ (cm^{-1})
BZ-O30-1a	Bize-Tournal	Unit IV, Layer G	15 ka	Cal	−	0.26	4.0	1.31	1.20	0.25	962.5
BZ-O30-1b	Bize-Tournal	Unit IV. Layer G	15 ka	Cal	−	0.26	3.8	1.34	1.18	0.25	963.0
BZ-O30-2	Bize-Tournal	Unit IV. Layer G	15 ka	Cal	−	0.05	8.6	2.31	1.58	0.11	963.0
BZ-O30-3	Bize-Tournal	Unit IV. Layer G	15 ka	Cal	−	0.05	8.0	1.93	1.61	0.12	962.6
BZ-O30-4	Bize-Tournal	Unit IV. Layer G	15 ka	Cha	−	0.27	3.8	1.21	1.18	0.26	961.6
BZ-O30-5	Bize-Tournal	Unit IV. Layer G	15 ka	Cha	−	0.29	3.5	1.22	1.18	0.24	961.5
BZ-O30-6	Bize-Tournal	Unit IV. Layer G	15 ka	Cha	−	0.21	3.7	1.19	1.18	0.27	961.2
BZ-O30-7	Bize-Tournal	Unit IV. Layer G	15 ka	UnH	−	0.22	3.7	1.25	1.19	0.25	961.4
BZ-O30-8	Bize-Tournal	Unit IV. Layer G	15 ka	UnH	0.14	0.29	3.7	1.17	1.17	0.29	961.5
BZ-O30-9	Bize-Tournal	Unit IV. Layer G	15 ka	UnH	0.18	0.26	3.6	1.13	1.17	0.32	960.7
BZ-O30-10	Bize-Tournal	Unit IV. Layer G	15 ka	UnH	0.13	0.26	3.7	1.20	1.18	0.28	961.4
BZ-O30-13	Bize-Tournal	Unit IV. Layer G	15 ka	UnH	−	0.25	3.5	1.20	1.17	0.26	960.9
BZ-O30-14	Bize-Tournal	Unit IV. Layer G	15 ka	UnH	−	0.25	3.6	1.22	1.19	0.25	961.0
BZ-O30-15	Bize-Tournal	Unit IV. Layer G	15 ka	UnH	0.06	0.27	3.7	1.16	1.19	0.28	961.1
BZ-O30-16	Bize-Tournal	Unit IV. Layer G	15 ka	UnH	0.07	0.27	3.7	1.19	1.18	0.27	961.4
BZ-O30-17	Bize-Tournal	Unit IV. Layer G	15 ka	UnH	0.22	0.33	3.5	1.12	1.16	0.33	961.0
BZ-O30-18	Bize-Tournal	Unit IV. Layer G	15 ka	UnH	0.10	0.29	3.7	1.19	1.17	0.29	961.5
BZ-O30-20	Bize-Tournal	Unit IV. Layer G	15 ka	Cal	−	0.17	4.1	1.41	1.19	0.26	962.7
BZ-O30-21	Bize-Tournal	Unit IV. Layer G	15 ka	Cha	−	0.23	3.9	1.27	1.19	0.24	961.9
BZ-O30-24	Bize-Tournal	Unit IV. Layer G	15 ka	Cal	−	0.05	8.9	2.34	1.50	0.13	963.3
BZ-O30-25a	Bize-Tournal	Unit IV. Layer G	15 ka	Cal	−	0.28	3.7	1.20	1.18	0.26	961.7
BZ-O30-25b	Bize-Tournal	Unit IV. Layer G	15 ka	Cha	−	0.27	3.8	1.22	1.18	0.26	961.9
BZ-O30-26	Bize-Tournal	Unit IV. Layer G	15 ka	Cal	−	0.04	9.4	2.44	1.64	0.10	963.1
Org-1	Orgnac 3	Layer 6	360 ka	Cal	−	0.02	10.5	2.61	1.75	0.09	963.2
Org-2	Orgnac 3	Layer 6	360 ka	UnH	−	0.24	3.6	1.23	1.18	0.25	961.1
Org-3	Orgnac 3	Layer 6	360 ka	UnH	−	0.27	3.8	1.25	1.20	0.25	961.6
Org-4	Orgnac 3	Layer 6	360 ka	UnH	−	0.20	3.9	1.27	1.21	0.25	961.5
Org-5	Orgnac 3	Layer 6	360 ka	Cha	−	0.25	3.7	1.22	1.18	0.25	961.6
Org-6	Orgnac 3	Layer 6	360 ka	Cha	−	0.24	3.9	1.26	1.20	0.24	961.9
Org-7	Orgnac 3	Layer 6	360 ka	Cha	−	0.28	3.7	1.20	1.17	0.26	961.8
Org-8	Orgnac 3	Layer 6	360 ka	Cal	−	0.04	7.9	1.95	1.62	0.14	962.6
Org-9	Orgnac 3	Layer 6	360 ka	UnH	−	0.26	3.5	1.17	1.18	0.27	960.6
Org-10	Orgnac 3	Layer 6	360 ka	Cha	−	0.27	4.4	1.38	1.26	0.22	962.5
Org-11	Orgnac 3	Layer 2	320 ka	Cal	−	0.27	3.5	1.23	1.18	0.27	961.5
Org-12	Orgnac 3	Layer 2	320 ka	Cal	−	0.15	4.9	1.64	1.25	0.22	962.8
Org-13	Orgnac 3	Layer 2	320 ka	UnH	−	0.27	3.7	1.24	1.18	0.26	961.8
Org-14	Orgnac 3	Layer 2	320 ka	Cal	−	0.18	4.2	1.37	1.21	0.23	962.3
Org-15	Orgnac 3	Layer 2	320 ka	Cha	−	0.24	3.8	1.23	1.18	0.26	961.9
Org-16	Orgnac 3	Layer 2	320 ka	Cal	−	0.20	3.9	1.35	1.20	0.24	962.1
Org-17	Orgnac 3	Layer 2	320 ka	Cal	−	0.04	9.7	2.71	1.71	0.10	963.3
ST-Ta-1a	Song Terus	Tabuhan layers	30−80 ka	UnH	−	0.31	3.5	1.38	1.18	0.25	963.0
ST-Ta-1b	Song Terus	Tabuhan layers	30−80 ka	UnH	−	0.24	3.3	1.35	1.18	0.26	962.7
ST-Ta-2	Song Terus	Tabuhan layers	30−80 ka	UnH	−	0.24	4.3	1.31	1.21	0.26	962.0
ST-Ta-3a	Song Terus	Tabuhan layers	30−80 ka	Cal	−	0.03	9.2	2.11	1.80	0.09	962.7
ST-Ta-3b	Song Terus	Tabuhan layers	30−80 ka	Cha	−	0.13	4.4	1.57	1.27	0.20	962.9
ST-Ta-4a	Song Terus	Tabuhan layers	30−80 ka	Cal	−	0.18	3.6	1.38	1.21	0.25	962.6
ST-Ta-4b	Song Terus	Tabuhan layers	30−80 ka	Cha	−	0.22	3.4	1.30	1.18	0.24	962.3
ST-Ta-6	Song Terus	Tabuhan layers	30−80 ka	Cha	−	0.23	3.7	1.36	1.20	0.21	962.3
ST-Ta-7a	Song Terus	Tabuhan layers	30−80 ka	UnH	−	0.24	3.3	1.33	1.17	0.25	963.3
ST-Ta-7b	Song Terus	Tabuhan layers	30−80 ka	UnH	−	0.24	3.3	1.35	1.17	0.26	963.6
ST-Ta-8	Song Terus	Tabuhan layers	30−80 ka	UnH	−	0.27	3.2	1.37	1.17	0.24	963.3
ST-Ta-9a	Song Terus	Tabuhan layers	30−80 ka	Cha	−	0.25	3.1	1.28	1.16	0.25	962.2
ST-Ta-10	Song Terus	Tabuhan layers	30−80 ka	UnH	−	0.24	4.1	1.40	1.21	0.23	963.1
ST-Ta-11	Song Terus	Tabuhan layers	30−80 ka	Cal	−	0.24	3.9	1.28	1.19	0.25	962.2
ST-Ta-12a	Song Terus	Tabuhan layers	30−80 ka	Cal	−	0.03	9.8	2.28	1.70	0.10	963.0
ST-Ta-12b	Song Terus	Tabuhan layers	30−80 ka	Cha	−	0.14	4.6	1.51	1.26	0.21	962.6
ST-Ta-13	Song Terus	Tabuhan layers	30−80 ka	UnH	−	0.19	4.5	1.39	1.23	0.23	962.3
ST-Ta-15	Song Terus	Tabuhan layers	30−80 ka	Cha	−	0.27	3.7	1.28	1.18	0.24	962.5
ST-Ta-16a	Song Terus	Tabuhan layers	30−80 ka	UnH	−	0.21	4.1	1.40	1.23	0.22	962.6
ST-Ta-17	Song Terus	Tabuhan layers	30−80 ka	UnH	−	0.23	4.1	1.38	1.20	0.24	962.5
ST-Ta-18	Song Terus	Tabuhan layers	30−80 ka	UnH	−	0.58	3.9	1.34	1.19	0.24	962.9
ST-Ta-20	Song Terus	Tabuhan layers	30−80 ka	UnH	−	0.28	3.9	1.33	1.18	0.26	963.1
ST-Ta-21	Song Terus	Tabuhan layers	30−80 ka	UnH	−	0.35	3.8	1.39	1.19	0.23	963.3
ST-Ta-22	Song Terus	Tabuhan layers	30−80 ka	UnH	−	0.25	4.1	1.36	1.20	0.24	962.8
ST-Ta-23a	Song Terus	Tabuhan layers	30−80 ka	Cal	−	0.03	9.5	2.15	1.75	0.10	962.7
ST-Ta-23b	Song Terus	Tabuhan layers	30−80 ka	Cal	−	0.12	5.2	1.61	1.30	0.20	962.6
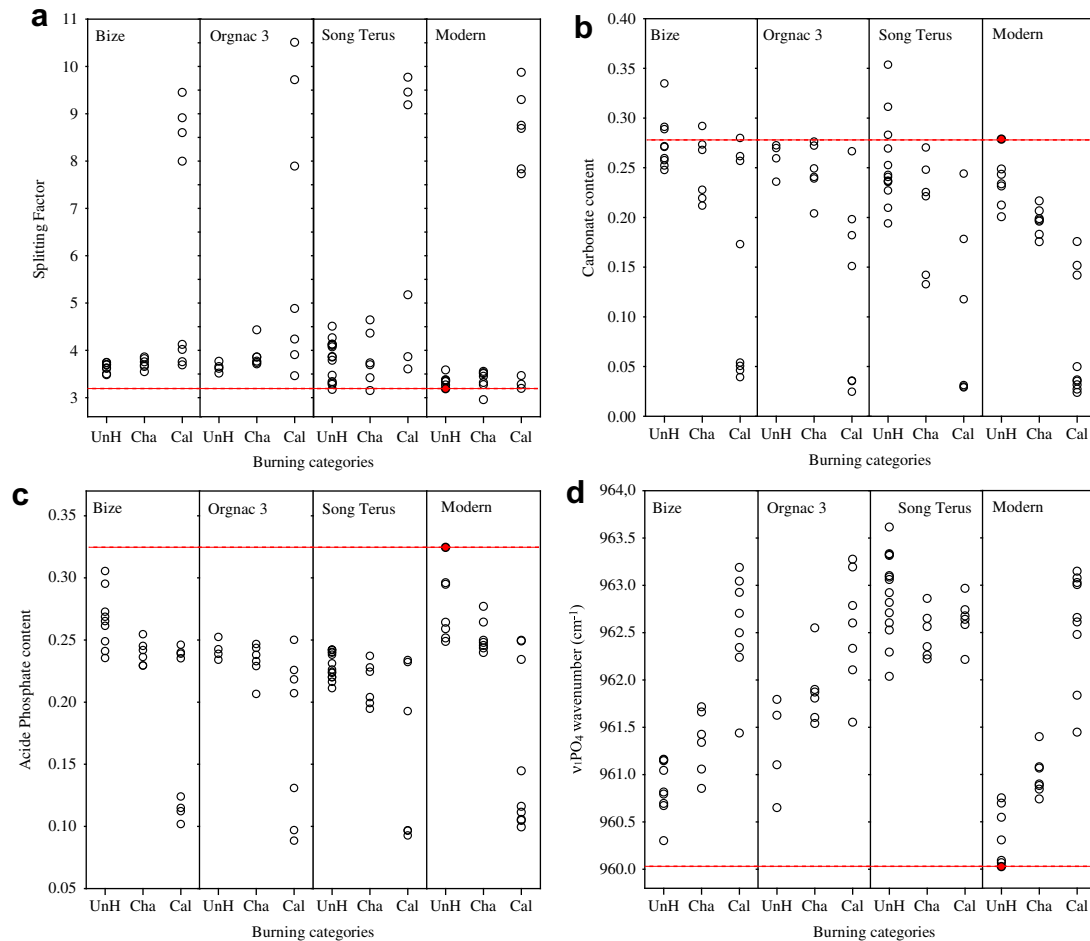
Fig. 4. a) Crystallinity (IRSF), b) carbonate content, c) acid phosphate content, and ν_1PO_4 band position for unheated (UnH), charred (Cha), and calcined (Cal) samples from Bize-Tournal Cave, Orgnac 3 and Song Terus Cave. Values observed for archaeological samples are compared with modern bones grouped in equivalent categories. Red dots and red lines refer to the values observed for an unheated modern sample. (For interpretation of the references to colour in this figure legend, the reader is referred to the web version of this article.)

similar IRSF values. No direct relationship can be observed between the preservation of a substantial amount of collagen and the crystallinity of these archaeological samples as is seen in several samples from Bize-Tournal.

Unheated samples from Song Terus exhibited scattered crystallinity values, and the IRSF values did not seem to reliably reflect their preservation state. Some of these samples had a high F content but showed IRSF values, which were similar, or even lower, than modern bones (e.g. for ST-Ta-1b and ST-Ta-7). As F⁻ uptake is known to induce a crystallinity increase, this observation could be ascribed to: (1) a lack of correlation between the crystallinity (crystal perfection and size) and the trace elements uptake (Pucéat et al., 2004; Trueman et al., 2008); (2) a lack of meaning of the IRSF measure to evaluate the crystallinity; or (3) an artificial decrease of crystallinity induced by sample preparation, for example during the grinding procedure (Nakano et al., 2002; Surovell and Stiner, 2001). This last hypothesis seems less probable because, if the crystallinity decrease was induced by the grinding of the sample, a significant increase of the acid phosphate content and a shift of the ν_1PO_4 might be observed. Fluoride uptake could also have modified the spectral feature of the ν_4PO_4 domain, and more particularly the relative peak intensities of the band at 605 and 565 cm⁻¹ (Weiner et al., 1993). Such changes could have affected the IRSF determination and limited the reliable evaluation of crystal size and perfection. However, the influence of

a F⁻ uptake on IRSF values seems complex: two samples can present the same F⁻ content but very different IRSF values (e.g. ST-Ta-1 and ST-Ta-10, F% = 1.7, IRSF respectively 3.5 and 4.1). Thus, these results confirm that IRSF cannot be used as an unequivocal proxy of the extent of diagenetic alteration (Chadefaux and Reiche, 2009; Pucéat et al., 2004; Reiche et al., 2002b; Trueman et al., 2008).

5.2.2. Evolution of acid phosphate content

Diagenetic processes seem to also influence the acid phosphate content, tending to progressively remove HPO_4^{2-} and non-apatitic environments (Cazalbou et al., 2004). HPO_4^{2-} amounts for altered samples fell in the range of values observed for modern bones heated around 550–600 °C (Fig. 4c). Unheated samples from Orgnac and Song Terus showed lower HPO_4^{2-} contents than the Bize-Tournal specimens. For unheated categories of Bize-Tournal samples, the highest acid phosphate contents were observed for fossil bones with preserved collagen. This result confirms that the mineral matter was protected from physico-chemical alteration by collagen (Trueman et al., 2008). As observed for modern heated samples, such a decrease in non-apatitic environments could also be related to the removal of the hydrated layers on the crystallite surface.

Cazalbou et al. (2004) mentioned that this decrease of HPO_4^{2-} and non-apatitic environments in the hydrated surface layer
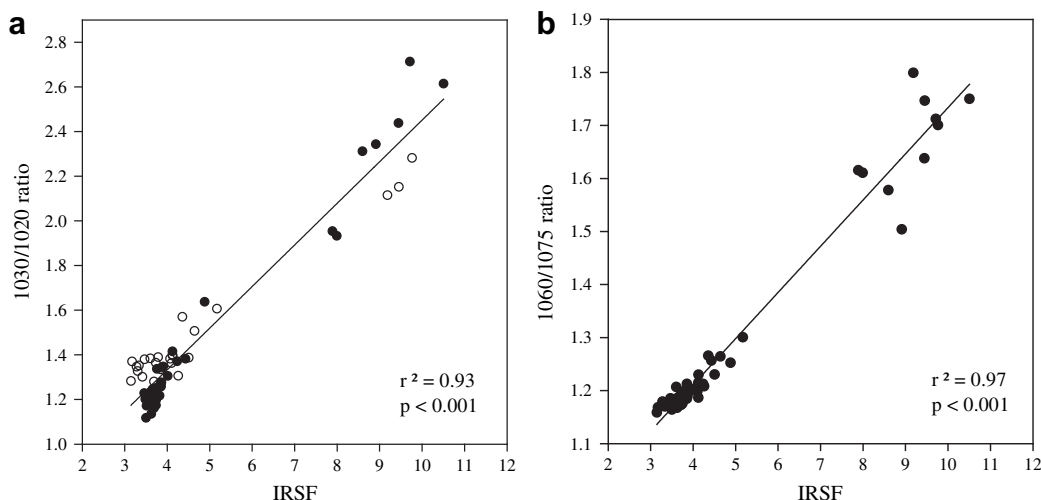
Fig. 5. a) Relationship between IRSF and 1030/1020 ratio for archaeological samples ($r^2 = 0.93$, $p < 0.001$). White dots correspond to Song Terus samples excluded from the calculation of the linear regression. b) Relationship between IRSF and 1060/1075 ratio ($r^2 = 0.97$, $p < 0.001$). For the two graphs, the dotted lines present the relationship observed for modern samples.

constitutes one of the first events occurring in bone mineral during diagenesis. This phenomenon could arise without any major restructuring of the mineral phase, and could allow the incorporation of foreign ions.

This process, however, seems to persist and to intensify with time. The more drastic decrease of HPO_4^{2-} content could, therefore, result from a dissolution and recrystallization process that favors crystal growth and thus decreases the specific surface area.

5.2.3. Position shift of ν_1PO_4 vibration band

The position of the ν_1PO_4 band of unheated and charred bones seems to undergo a shift during diagenesis. Following the hypothesis presented above for the experimentally heated samples, this increase in the frequency of the ν_1PO_4 band might testify to a decrease in lattice strain and more ordered atomic arrangement of the apatite lattice. This hypothesis can be confirmed by the analyses performed on the Song Terus samples which exhibit a high frequency for the ν_1PO_4 band. Some of these unheated samples showed a higher position of the ν_1PO_4 band than for pure HA (usually around 963 cm^{-1}). Such position shift may be explained by high F$^-$ contents in these samples. Previous papers have reported similar elevated positions of this band for fluorapatite (FA) or carbonate fluorapatite (francolite) compared with HA (Antonakos

et al., 2007; Penel et al., 1997; Thomas et al., 2007). The F$^-$ uptake in fossil bones and teeth has been extensively investigated in the past for the purpose of relative dating and as a proxy of diagenetic alteration (Ikeya, 1985; Michel et al., 1996; Reiche et al., 1999, 2002b). The incorporation of F$^-$ by substitution for OH$^-$ ions causes a contraction in the a-axis dimension that promotes a more ordered atomic arrangement in the apatitic unit cell of FA compared to HA and promotes crystal growth (LeGeros, 1981; Michel et al., 1996). The results obtained for fossil bones indicate that the spectral position of the ν_1PO_4 band can provide further information on compositional changes in the mineral phase associated with increased atomic order in the apatite lattice.

6. Alteration process of unheated and charred bones vs calcined bones

The comparison of the diagenetic structural and chemical modifications occurring over the different heating categories of fossil bones shows that the extent of *post-mortem* alteration depends on the initial stage of burning. Unheated and charred bones were more altered by diagenetic processes than calcined samples. Moreover, the rapid transformation of the mineral phase occurring between 500 and 700 °C leads to the formation of two

Table 4
Major. minor and trace element concentrations in the archaeological bone samples from Bize-Tournal Cave, Orgnac 3 and Song Terus Cave obtained by PIXE/PIGE analysis. Mean element oxide concentrations are expressed in ppm except for P, Ca and F (wt%). Mean statistical error varies between 5 and 10 wt%.

	Heating stage	P_2O_5 (%)	CaO (%)	Na_2O (ppm)	MgO (ppm)	SO_3 (ppm)	Al_2O_3 (ppm)	SiO_2 (ppm)	ZnO (ppm)	SrO (ppm)	Cl (ppm)	MnO (ppm)	Fe_2O_3 (ppm)	CuO (ppm)	BaO (ppm)	F (%)
Modern				8500	7800	1600	–	–	130	250	750	–	–	–	–	0.05
BZ-9	UnH	39.6	58.8	6592	4086	2454	2944	0	522	465	267	13	44	920	334	0.3
BZ-13	UnH	39.2	59.2	6870	4207	2877	1531	0	365	330	199	22	54	858	228	0.2
BZ-15	UnH	38.8	59.7	6001	3239	2455	1550	0	706	313	108	39	88	795	68	0.3
BZ-17	UnH	38.8	59.6	7037	3461	3315	1478	0	326	339	316	31	50	874	186	0.5
Org-2	UnH	40.5	56.5	5209	2361	1782	9429	8287	716	272	255	381	820	142	276	0.0
Org-6	Cha	38.7	59.6	7213	2202	2412	3384	0	387	156	1816	159	337	1097	138	0.9
Org-8	Cal	42.8	56.1	3863	899	1301	2341	1041	83	139	829	36	474	6	224	0.1
Org-9	UnH	38.0	60.6	5542	2117	2707	2304	0	447	271	572	8	172	933	143	0.9
Org-10	Cha	36.9	59.4	5917	788	3495	7014	3599	200	75	4073	131	1659	282	314	0.8
ST-Ta-1	UnH	37.5	60.9	6182	2989	2114	1361	0	156	909	1070	1121	977	797	523	1.7
ST-Ta-2	UnH	39.3	57.5	4530	2647	2022	7599	9528	159	1361	356	1588	4372	32	610	1.4
ST-Ta-3	Cal	42.2	56.5	6851	1872	998	612	0	69	448	1318	111	107	22	313	0.6
ST-Ta-7	UnH	39.4	58.8	5554	2303	1281	2699	5252	134	731	258	54	95	27	573	1.8
ST-Ta-10	UnH	38.5	59.9	5274	2869	2399	1797	327	162	1218	317	1515	1673	843	540	1.7

kinds of calcined bones: grey to light grey bones displaying low crystallinity, and white bones that exhibit high crystallinity. These highly crystalline samples, undoubtedly heated to at least 650 °C, undergo only weak modifications of their elemental composition, crystallinity, carbonate and acid phosphate contents during diagenesis, and remain in the range observed for modern calcined bones. The more limited F$^-$ uptake process in calcined bones also prevents the position shift of the v_1PO$_4$ band (e.g. samples Org8 and St-Ta-2). This specific pattern can be explained by the loss of structural carbonate and by the growth of crystallites at temperatures higher than 650 °C that reduces the reactivity of the mineral phase and prevents compositional and structural properties from experiencing severe diagenetic modifications (Lanting et al., 2001; Lebon, 2008; Reiche et al., 2002a).

The structural properties acquired by bone mineral matter heated over 600 °C increase the structural stability of the mineral phase in burial environments. Moreover, such properties are clearly distinct from those induced by low temperature heating or diagenetic processes and allow a reliable identification of archaeological samples exposed to high temperatures by FTIR.

In contrast, low temperature heating and diagenesis seem to produce similar effects on the mineral matter, even if different physico-chemical processes are involved. This could limit the possibilities of using the mineral properties to identify burnt bones in archaeological contexts if the samples are diagenetically altered.

6.1. Further combined FTIR proxies to better characterize diagenetic alterations

The IRSF alone seems to fail to describe the complexity of the alteration processes occurring in bone mineral during diagenesis, and thus cannot provide a complete evaluation of bone preservation state. However, the further proxies developed in this study, easily obtained from the several sub-bands of the v_1v_3PO$_4$ domain, could contribute to provide a more precise view of the alteration state of fossil bones.

The progressive decrease of acid phosphate content constitutes one of these proxies. As an example, the results of Song Terus are discussed in detail. The altered unheated samples from Song Terus cave clearly presented lower HPO$_4^{2-}$ content than modern bones, whereas some of them displayed IRSF values very similar to modern samples.

This was also the case for the frequencies of the v_1PO$_4$ vibration band. The F$^-$ uptake highlighted in the Song Terus samples did not seem to have affected the crystallinity of the overall unheated and charred bones, whereas the v_1PO$_4$ position clearly demonstrates major changes of the crystal perfection. Based on the shift of this band in apatite doped with Ba^{2+}, Mn^{2+}, Sr^{2+}, or F$^-$ ions, use of the band position has been proposed as a proxy to detect ionic substitutions in mineral lattice during fossilization. This different behavior observed for IRSF and v_1PO$_4$ position probably results from a differential sensitivity of both spectroscopic indices to the multiple processes of composition and structural modifications affecting the bones during burial. As previously noted by Trueman et al. (2004), IRSF seems to be directly related to the mean crystal length, meaning that it cannot reflect alone the crystallinity defined as crystallite size and perfection. The perfection of apatite crystals could be more sensitively evaluated by the v_1PO$_4$ positive shift which is related to the more ordered atomic arrangement in the lattice, induced for example by decrease in CO$_3^{2-}$ content or uptake of F$^-$. However, the incorporation of bivalent ions such as Sr^{2+}, Ba^{2+} Mn^{2+} Fe^{2+} as substituents for Ca^{2+} in the apatite lattice could also result in changes in lattice parameters and a reduction of the crystallinity (LeGeros, 1981). Thomas et al. (2007), indicated that apatites doped with Ba^{2+}, Mn^{2+}, of Sr^{2+} exhibited a lower frequency for the v_1PO$_4$ band. Further investigation is needed to better understand the consequences on HA lattice order and v_1PO$_4$ frequency of a conjoint incorporation of ions which would individually have opposite effects on these parameters. The elemental composition determined by μPIXE/PIGE analysis has notably yield valuable information to understand the origin of the structural changes of bone mineral observed during burial. The generalization of μPIXE/PIGE analysis could hence help to a better understanding of spectroscopic changes related to mineral matter modifications occurring during burial.

We also note that the crystallinity indices obtained from the v_1v_3PO$_4$ and the v_4PO$_4$ domains seem to represent different aspects of the alteration process. Similar linear correlation can be observed between the 1060/1075 ratio and IRSF for both modern and fossil samples. This was not the case for the 1030/1020 ratio for which the relationship with the IRSF was different for modern and fossil bones. Furthermore, the relationship between the 1030/1020 ratio and IRSF for Song Terus samples differed from those observed for the other fossil bones. This suggests different behaviors of these two indices depending on the specific alteration processes affecting
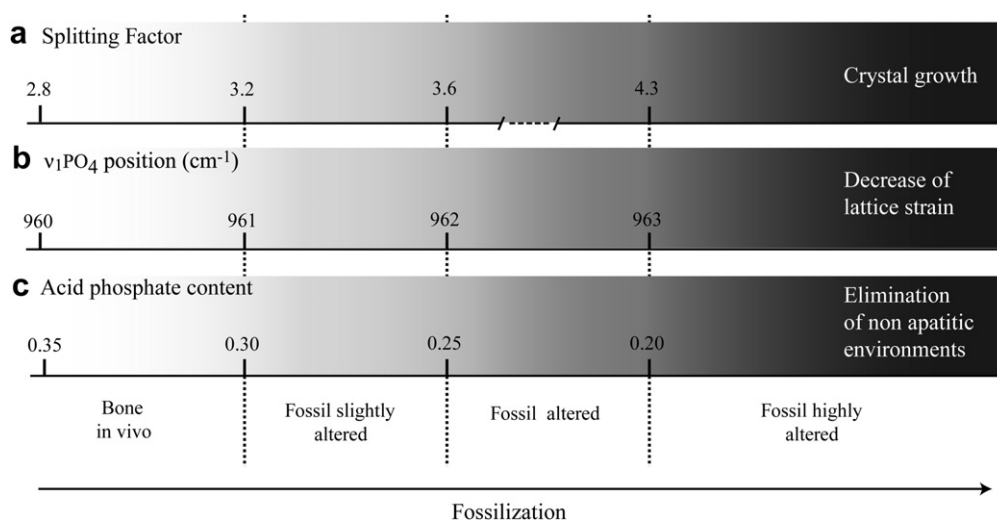

Fig. 6. a) Evaluation of the alteration stage of mineral matter of fossil bone by the combination of the crystallinity (IRSF) adapted from Berna et al. (2004), b) The position of the v_1PO$_4$ band (atomic order in the apatitic lattice related to ionic substitution), and c) acid phosphate content (elimination of non-apatitic environments).

the Song Terus bone remains, especially F$^-$ uptake. More detailed investigations of the modifications affecting these spectral domains during diagenesis are therefore required.

Finally, all results obtained for the fossil bones have been discussed in comparison with those obtained for one modern ox bone, without regarding to its maturity and health. These parameters, as well as species or anatomical origin of the skeletal remains being studied, could influence the initial values of the proxies prior to diagenetic processes. The character of the modern reference material must be considered when analyzing intra- and inter-subject variability of bone composition.

Nevertheless, all these observations suggest that the measurements of the $\nu_1 PO_4$ peak frequency and of the acid phosphate content can efficiently contribute to a more precise view of the alteration stages of fossil bones by FTIR (Fig. 6). These proxies should now be applied to unheated samples to see whether they can predict the preservation state of the isotopic and elemental biogenic signals more efficiently than IRSF. Associated with other alteration proxies such as organic matter preservation, carbonate content, secondary mineral deposits and porosity measurements, theses indices could thus contribute to a more efficient evaluation of state of preservation of bone samples prior to engaging in expensive and longer analyses.

7. Conclusion

Despite the various time scales over which they occur, low temperature heating and diagenetic processes may induce similar modifications of the mineral structure and composition of bones. These processes are, however, clearly distinct from those induced by high temperature heating, suggesting that only burning temperatures greater than 550 °C can be clearly recognized from studies of the mineral composition of archaeological bone. The simultaneous study of experimental heating and the comparison between unburnt and burnt archaeological samples provides us useful information on diagenetic processes. The analytical approach developed by FTIR measurement and exploitation of the $\nu_1 \nu_3 PO_4$ domain of artificially heated modern bones allows us to define and calibrate different indices reflecting the composition and the structure of mineral matter composition. Crystallinity is recorded both by the ν_4 domain (IRSF) and the $\nu_1 \nu_3$ domain (1030/1020 and 1060/1075 ratios). As previously documented by Pucéat et al. (2004) and Trueman et al. (2008), the classical measure of crystallinity alone proves to be far from sufficient to describe post-mortem alterations, although its association with other proxies such as the frequency of $\nu_1 PO_4$ band and the acid phosphate content seems to efficiently complete it. The $\nu_1 PO_4$ band frequency seems to be directly related to the perfection of atomic arrangement in the mineral lattice, and could be used to identify modifications of chemical composition that enhance order in this lattice, as for example by F$^-$ uptake. The acid phosphate content can be used to monitor the elimination of "non-apatitic" environments occurring during the first stage of the alteration of bone mineral matter. These new spectroscopic indices can be easily obtained from FTIR spectra to screen for diagenetic alteration. Furthermore, these indices, measured from the $\nu_1 \nu_3 PO_4$ domain offer the additional advantage of being accessible in micro-FTIR spectroscopy contrary to the ν_4 domain that is outside the detection range of most micro-FTIR detector devices. The spectroscopic indices developed here will offer a substantially improved ability to understand the alteration processes undergone by fossil bone mineral; an opportunity that might even be developed at the histological scale using micro-FTIR (Reiche et al., in preparation).

Acknowledgments

References

Antonakos, A., Liarokapis, E., Leventouri, T., 2007. Micro-Raman and FTIR studies of synthetic and natural apatites. Biomaterials 28, 3043–3054.

Berna, F., Matthews, A., Weiner, S., 2004. Solubilities of bone mineral from archaeological sites: the recrystallization window. Journal of Archaeological Science 31, 867–882.

Biltz, R.M., Pellegrino, E.D., 1983. The composition of recrystallized bone mineral. Journal of Dental Research 62 (12), 1190–1195.

Bocherens, H., Drucker, D.G., Billiou, D., Geneste, J.-M., Kervazo, B., 2008. Grotte Chauvet (Ardèche, France): a "natural experiment" for bone diagenesis in karstic context. Palaeogeography, Palaeoclimatology, Palaeoecology 266 (3–4), 220–226.

Boskey, A., Pleshko-Camacho, N., 2007. FT-IR imaging of native and tissue-engineered bone and cartilage. Biomaterials 28, 2465–2478.

Calligaro, T., Dran, J.C., Salomon, J., Walter, P., 2004. Review of accelerator gadgets for art and archaeology. Nuclear Instruments and Methods in Physics Research B 226, 9–37.

Cazalbou, S., Eichert, D., Drouet, C., Combes, C., Rey, C., 2004. Minéralisations biologiques à base de phosphates de calcium. Comptes Rendus Palevol 3, 563–572.

Chadefaux, C., Le Hô, A.-S., Bellot-Gurlet, L., Reiche, I., 2009. Micro-ATR-FT-IR and micro-FT-Raman studies on archaeological bone materials from the lake site of Chalain (France). Proceedings IRUG 6, 129–137.

Chadefaux, C., Reiche, I., 2009. Archaeological bone from macro- to nanoscale. Heat-induced modifications at low temperatures. Journal of Nano Research 8, 157–172.

Collins, M.J., Nielsen-Marsh, C.M., Hiller, J., Smith, C.I., Roberts, J.P., Prigodich, R.V., Wess, T.J., Csapo, J., Millard, A.R., Turner-Walker, G., 2002. The survival of organic matter in bone: a review. Archaeometry 44, 383–394.

Currey, J.D., 2006. Bones: Structure and Mechanics. Princeton University Press. 456 pp.

Eichert, D., Salomé, M., Banu, M., Susini, J., Rey, C., 2005. Preliminary characterization of calcium chemical environment in apatitic and non-apatitic calcium phosphates of biological interest by X-ray absorption spectroscopy. Spectrochimica Acta Part B: Atomic Spectroscopy 60 (6), 850–858.

Elliott, J.C., 2002. Calcium phosphate biominerals. In: Kohn, M.J., Rakovan, J., Hughes, J.M. (Eds.), Phosphates: Geochemical, Geobiological, and Materials Importance. Reviews in Mineralogy & Geochemistry, pp. 427–453.

Eppell, S.J., Tong, W., Katz, J.L., Kuhn, L., Glimcher, M.J., 2001. Shape and size of isolated bone mineralites measured using atomic force microscopy. Journal of Orthopaedic Research 19 (6), 1027–1034.

Etok, S.E., Valsami-Jones, E., Wess, T.J., Hiller, J.C., Maxwell, C.A., Rogers, K.D., Manning, D.A.C., White, M.L., Lopez-Capel, E., Collins, M.J., et al., 2007. Structural and chemical changes of thermally treated bone apatite. Journal of Materials Science 72, 9807–9816.

Falguères, C., Shen, G., Yokoyama, Y., 1988. Datation de l'Aven d'Orgnac III: comparaison par les méthodes de la résonnance de spin électronique et du déséquilibre des familles de l'uranium. L'Anthropologie 92, 727–729.

Fröhlich, F., 1989. Deep-sea biogenic silica: new structural and analytical data from infrared analysis − geological implications. Terra Nova 1, 267–273.

Gadaleta, S.J., Paschalis, E.P., Betts, F., Mendelsohn, R., Boskey, A.L., 1996. Fourier transform infrared spectroscopy of the solution-mediated conversion of amorphous calcium phosphates to hydroxyapatite: new correlations between X-ray diffraction and infrared data. Calcified Tissue International 58, 9–16.

Grün, R., 1989. Electron spin resonance (ESR) dating. Quaternary International 1, 65–109.

Hameau, S., Falguères, C., Bahain, J.J., Sémah, F., Sémah, A.M., Dolo, J.M., 2007. ESR dating in Song Terus cave (East Java, Indonesia). Quaternary Geochronology 2 (1–4), 398–402.

Hedges, R.E.M., 2002. Bone diagenesis: an overview of processes. Archaeometry 44, 319–328.

Hedges, R.E.M., Millard, A.R., 1995. Bones and groundwater: towards the modelling of diagenetic processes. Journal of Archaeological Science 22, 155–164.

Hedges, R.E.M., Millard, A.R., Pike, A.W.G., 1995. Measurements and relationships of diagenetic alteration of bone from three archaeological sites. Journal of Archaeological Science 22, 201–209.

Holcomb, D.W., Young, R.A., 1980. Thermal decomposition of human enamel. Calcified Tissue International 31, 189–201.

Ikeya, M., 1985. ESR ages of bones in paleo-anthropology: uranium and fluorine accumulation. In: Ikeya, M., Miki, T. (Eds.), First International Symposium on ESR Dating. Ionics, Tokyo, Ube-Akiyoshi, Yamaguchi, Japan, pp. 373–379.

Jans, M.M.E., Kars, H., Nielsen-Marsh, C.M., Smith, C.I., Nord, A.G., Arthur, P., Earl, E., 2002. In situ preservation of archaeological bone: a histology study within a multidisciplinary approach. Archaeometry 44, 343–352.

Lanting, J.N., Aerts-Bijma, A.T., van der Plicht, J., 2001. Dating cremated bone. Radiocarbon 43 (2A), 249–254.

Lebon, M., 2008. Caractérisation par Spectroscopie Infrarouge à Transformée de Fourier des ossements chauffés en contexte archéologique – Comparaison entre référentiel moderne et matériel archéologique, Implication diagénétique. Thèse du Muséum national d'Histoire naturelle, Paris, 339 pp.

Lebon, M., Reiche, I., Fröhlich, F., Bahain, J.J., Falguères, C., 2008. Characterization of archaeological burnt bones: contribution of a new analytical protocol based on derivative FTIR spectroscopy and curve fitting of the $\nu_1 \nu_3 PO_4$ domain. Analytical and Bioanalytical Chemistry 392 (7), 1479–1488.

Lee-Thorp, J., 2002. Two decades of progress towards understanding fossilization processes and isotopic signals in calcified tissue minerals. Archaeometry 44 (3), 435–446.

Lee-Thorp, J., Sponheimer, M., 2003. Three case studies used to reassess the reliability of fossil bone and enamel isotope signals for paleodietary studies. Journal of Anthropological Archaeology 22 (3), 208–216.

LeGeros, R.Z., 1981. Apatites in biological system. Progress in Crystal Growth and Characterization 4, 1–45.

Legros, R., Balmain, N., Bonel, G., 1987. Age-related changes in mineral of rat and bovine cortical bone. Calcified Tissue International 41 (3), 137–144.

Magniez, P., 2009. Taphonomic study of the middle and upper palaeolothic large mammal assemblage from Tournal Cave (Bize-Minervois, France). Journal of Taphonomy 7 (2–3), 203–233.

Maxwell, J.A., Campbell, J.L., Teesdale, W.J., 1988. The Guelph PIXE software. A description of the code package. Nuclear Instruments and Methods in Physics Research B 43, 218–230.

Michel, V., Ildefonse, P., Morin, G., 1996. Assessment of archaeological bone and dentine preservation from Lazaret cave (Middle Pleistocene) in France. Palaeo 126, 109–119.

Miller, L.M., Vairavanurthy, V., Chance, M.R., Mendelsohn, R., Paschalis, E.P., Betts, F., Boskey, A.L., 2001. In situ analysis of mineral content and crystallinity in bone using infrared micro-spectrometry of the $\nu_4 PO_4^{3-}$ vibration. Biochimica et Biophysica Acta 1527, 11–19.

Munro, L.E., Longstaffe, F.J., White, C.D., 2007. Burning and boiling of modern deer bone: effects on crystallinity and oxygen isotope composition of bioapatite phosphate. Palaeogeography, Palaeoclimatology, Palaeoecology 249, 90–102.

Munro, L.E., Longstaffe, F.J., White, C.D., 2008. Effects of heating on the carbon and oxygen-isotope compositions of structural carbonate in bioapatite from modern deer bone. Palaeogeography, Palaeoclimatology, Palaeoecology 266 (3–4), 142–150.

Nakano, T., Tokumura, A., Umahoshi, Y., 2002. Variation in crystallinity of hydroxyapatite and the related calcium phosphates by mechanical grinding and subsequent heat treatment. Metallurgical and Materials Transactions A 33A, 521–528.

Nielsen-Marsh, C.M., Hedges, R.E.M., Mann, T., Collins, M.J., 2000. A preliminary investigation of the application of differential scanning calorimetry to the study of collagen degradation in archaeological bone. Thermochimica Acta 365 (1–2), 129–139.

Paschalis, E.P., DiCarlo, E., Betts, F., Sherman, P., Mendelsohn, R., Boskey, A.L., 1996. FTIR microspectroscopic analysis of human osteonal bone. Calcified Tissue International 59, 480–487.

Pasteris, J.D., Wopenka, B., Freeman, J.J., Rogers, K., Valsami-Jones, E., van der Houwen, J.A.M., Silva, M.J., 2004. Lack of OH in nanocrystalline apatite as a function of degree of atomic order: implications for bone and biomaterials. Biomaterials 25, 229–238.

Penel, G., Leroy, G., Rey, C., Sombret, B., Huvenne, J.P., Bres, E., 1997. Infrared and Raman microspectrometry study of fluor-fluor-hydroxy and hydroxy-apatite powders. Journal of Material Science: Material in Medecine 8, 271–276.

Person, A., Bocherens, H., Mariotti, A., Renard, M., 1996. Diagenetic evolution and experimental heating of bone phosphate. Palaeogeography, Palaeoclimatology, Palaeoecology 78, 37–54.

Person, A., Bocherens, H., Saliège, J.-F., Paris, F., Zeitoun, V., Gérard, M., 1995. Early diagenetic evolution of bone phosphate: an X-ray diffractometry analysis. Journal of Archaeological Science 22 (2), 211–221.

Pucéat, E., Reynard, B., Lécuyer, C., 2004. Can crystallinity be used to determine the degree of chemical alteration of biogenic apatites? Chemical Geology 205, 83–97.

Reiche, I., Favre-Quattropani, L., Calligaro, T., Salomon, J., Bocherens, H., Charlet, L., Menu, M., 1999. Trace element composition of archaeological bones and postmortem alteration in the burial environment. Nuclear Instruments and Methods in Physics Research B 150, 656–662.

Reiche, I., Favre-Quattropani, L., Vignaud, C., Bocherens, H., Charlet, L., Menu, M., 2003. A multi-analytical study of bone diagenesis: the Neolithic site of Bercy (Paris, France). Measurement Science and Technology 14, 1608–1619.

Reiche, I., Lebon, M., Chadefaux, C., Müller, K., Le Hô, A.-S., Gensch, M., Schade, U. Microscale imaging of the state of preservation of 5000-years-old archaeological bones by synchrotron infrared microspectroscopy. Analytical and Bioanalytical Chemistry, accepted.

Reiche, I., Vignaud, C., Favre-Quattropani, L., Menu, M., 2002a. Fluorine analysis in biogenic and geological apatite by analytical transmission electron microscopy and nuclear reaction analysis. Journal of Trace and Microprobe Techniques 20 (2), 211–231.

Reiche, I., Vignaud, C., Menu, M., 2002b. The crystallinity of ancient bone and dentine: new insights by transmission electron microscopy. Archaeometry 44, 447–459.

Rey, C., Combes, C., Drouet, C., Sfihi, H., Barroug, A., 2007. Physico-chemical properties of nanocrystalline apatites: implications for biominerals and biomaterials. Materials Science and Engineering: C 27 (2), 198–205.

Rey, C., Shimizu, M., Collins, B., Glimcher, M.J., 1990. Resolution-enhanced Fourier transform infrared spectroscopy study of the environment of phosphate ion in the early deposits of a solid phase of calcium phosphate in bone and enamel and their evolution with age: 1. Investigations in the $\nu_4 PO_4$ domain. Calcified Tissue International 46, 384–394.

Rey, C., Shimizu, M., Collins, B., Glimcher, M.J., 1991. Resolution-enhanced Fourier transform infrared spectroscopy study of the environment of phosphate ion in the early deposits of a solid phase of calcium phosphate in bone and enamel and their evolution with age: 2. Investigations in the $\nu_3 PO_4$ domain. Calcified Tissue International 49, 383–388.

Rogers, K.D., Daniels, P., 2002. An X-Ray diffraction study of the effects of heat treatment on bone mineral microstructure. Biomaterials 23, 2577–2585.

Schwarcz, H.P., 1997. Uranium series dating. In: Taylor, R.E., Aitken, M.J. (Eds.), Chronometric Dating in Archaeology. Plenum Press, New York.

Sémah, F., Sémah, A.-M., Falguères, C., Gallet, X., Hameau, S., Moigne, A.-M., Simanjuntak, H.T., 2004. The significance of the Punung karstic area (Eastern Java) for the chronology of the Javanese Palaeolithic, with special reference to the Song Terus cave. Modern Quaternary Research in Southeast Asia 18, 45–62.

Shemesh, A., 1990. Crystallinity and diagenesis of sedimentary apatites. Geochimica et Cosmochimica Acta 54 (9), 2433–2438.

Sponheimer, M., Lee-Thorp, J., 1999. Alteration of enamel carbonate environments during fossilization. Journal of Archaeological Science 26, 143–150.

Stiner, M.C., Kuhn, S.L., Weiner, S., Bar-Yosef, O., 1995. Differential burning recrystallization, and fragmentation of archaeological bone. Journal of Archaeological Science 22, 223–237.

Surovell, T.A., Stiner, M.C., 2001. Standardizing infra-red measures of bone mineral crystallinity: an experimental approach. Journal of Archaeological Science 28, 633–642.

Tavoso, A., 1987. Le remplissage de la grotte Tournal à Bize-Minervois (Aude). Cypsela, VI, Girona, 23–25.

Termine, J., Posner, A.S., 1966. Infra-red determination of the percentage of crystallinity in apatitic calcium phosphates. Nature 211, 268–270.

Thomas, D.B., Fordyce, R.E., Frew, R.D., Gordon, K.C., 2007. A rapid, non-destructive method of detecting diagenetic alteration in fossil bone using Raman spectroscopy. Journal of Raman Spectroscopy 38, 1533–1537.

Trueman, C.N., Privat, K., Field, J., 2008. Why do crystallinity values fail to predict the extent of diagenetic alteration of bone mineral? Palaeogeography, Palaeoclimatology, Palaeoecology 266 (3–4), 160–167.

Trueman, C.N.G., Behrensmeyer, A.K., Tuross, N., Weiner, S., 2004. Mineralogical and compositional changes in bones exposed on soil surfaces in Amboseli National Park, Kenya: diagenetic mechanisms and the role of sediment pore fluids. Journal of Archaeological Science 31, 721–739.

Turner-Walker, G., Syversen, U., 2002. Quantifying histological changes in archaeological bones using BSE-SEM image analysis. Archaeometry 3, 461–468.

Weiner, S., Bar-Yosef, O., 1990. States of preservation of bones from prehistoric sites in the near East: a survey. Journal of Archaeological Science 17, 187–196.

Weiner, S., Goldberg, P., Bar-Yosef, O., 1993. Bone preservation in Kebara cave, Israel using on-site Fourier transformation infrared spectrometry. Journal of Archaeological Science 20, 613–627.

Wopenka, B., Pasteris, J.D., 2005. A mineralogical perspective on the apatite in bone. Materials Science and Engineering: C 25, 131–143.

Wright, L.E., Schwarcz, H.P., 1996. Infrared and isotopic evidence for diagenesis of bone apatite at Dos Pilas, Guatemala: palaeodietary implications. Journal of Archaeological Science 23, 933–944.